Journal of Materials Chemistry C

ROYAL SOCIETY OF CHEMISTRY

PAPER

View Article Online
View Journal | View Issue

Cite this: J. Mater. Chem. C, 2025, 13, 3408

Photochromism and efficient photothermal conversion of B ← N Lewis adducts induced by intramolecular electron transfer†

Sotaro Kusumoto, *[a] Takuma Mio,[a] Kenta Rakumitsu, [b] Masaya Shimabukuro, [c] Mamiko Kobayashi,[c] Tomoya Fukui, [de] Nobutsugu Hamamoto,[f] Toshiharu Ishizaki, [g] Yang Kim[h] and Yoshihiro Koide*[a]

The unique potential of B ← N Lewis adducts, a series of compounds composed of triphenylborane and pyridine/pyrazine derivatives, was investigated, which exhibited both photochromism and remarkably high-efficiency photothermal conversion, as well as being easy to prepare. They exhibit photochromism by generating organic radicals through intramolecular electron transfer upon exposure to UV light (365 nm). This feature, which distinguishes it from other photochromic materials, allows them to function as photothermal conversion materials with high efficiency up to 82% under NIR (850 nm) irradiation, a significant leap over both inorganic and organic materials and coordination compounds. To our knowledge, this research is the first to demonstrate the potential of B ← N adducts as both photochromic and NIR photothermal materials, opening up their various applications in the future.

Received 26th August 2024,
Accepted 9th December 2024

DOI: 10.1039/d4tc03640a

rsc.li/materials-c

Introduction

Photothermal conversion materials, which generate heat by absorbing near-infrared (NIR, 780 nm to 1300 nm) light, are used in various applications, including photothermal therapy,[1] diagnostics,[2] and night vision sensors.[3] However, current organic photothermal conversion materials[4] – such as indocyanine green,[5] heptamethine,[6] cyanine dyes,[7] phthalocyanines,[8] porphyrins,[9] pyrroles,[10] and croconaine dye[11] – face significant limitations. Recently, there have been reports on strong donor–acceptor type organic small molecules[12] and polymers[13] designed to enhance near-infrared absorption. However, as indicated in previous studies,[4–11] these materials—especially the aforementioned π-conjugated molecules—require complex molecular designs. This complexity often leads to lengthy synthesis processes, hindering further advancements in photothermal conversion material research. Therefore, there is a pressing need to develop more straightforward materials that are easy to synthesize and demonstrate improved photothermal conversion capability.

Photochromic materials prepared based on methyl viologen,[14] zwitterionic coordination polymers,[15] polyoxometalates,[16] naphthalene diimides,[17] and perylene diimides[18] have attracted attention for their applications in decoration, display, information storage, and anti-counterfeiting fields.[19] They have been extensively studied for photochromism driven by intermolecular electron transfer between donor and acceptor moieties, as materials capable of generating organic radicals. Some exhibit NIR absorption bands, making them potential candidates for photothermal transformation applications.[20] The photochromic properties often depend on intermolecular electron transfer, but this can also introduce uncertainties in photochromism due to their molecular arrangement. Therefore, it remains a challenge to develop photochromic materials that are easy to synthesize, exhibit NIR absorption bands through intramolecular charge transfer, and achieve high radical stability in photothermal conversion applications.

[a] Department of Applied Chemistry, Faculty of Chemistry and Biochemistry, Kanagawa University, 3-27-1 Rokkakubashi, Kanagawa-ku, Yokohama 221-8686, Japan. E-mail: kusumoto@kanagawa-u.ac.jp, ykoide01@kanagawa-u.ac.jp
[b] Graduate School of Pharmaceutical Sciences, Chiba University, 1-8-1 Inohana, Chuo-ku, Chiba 260-8675, Japan
[c] Institute of Biomaterials and Bioengineering, Tokyo Medical and Dental University, 2-3-10, Kanda-Surugadai, Chiyoda-ku, Tokyo 101-0062, Japan
[d] Laboratory for Chemistry and Life Science, Institute of Innovative Research, Tokyo Institute of Technology, 4259 Nagatsuta-cho, Midori-ku, Yokohama, Kanagawa 226-8501, Japan
[e] Research Center for Autonomous Systems Materialogy (ASMat), Institute of Innovative Research, Tokyo Institute of Technology, 4259 Nagatsuta-cho, Midori-ku, Yokohama, Kanagawa 226-8501, Japan
[f] Department of Applied Chemistry, Faculty of Engineering, Sanyo-Onoda City University, Sanyo-Onoda, Yamaguchi 756-0884, Japan
[g] Department of Chemistry, College of Humanities and Sciences, Nihon University, 3-25-40 Sakurajosui, Setagaya-ku, Tokyo 156-8550, Japan
[h] Department of Chemistry, Graduate School of Science and Technology, Kumamoto University, 2-39-1 Kurokami, Chuo-ku, Kumamoto 860-8555, Japan

† Electronic supplementary information (ESI) available. CCDC 2379690–2379694. For ESI and crystallographic data in CIF or other electronic format see DOI: https://doi.org/10.1039/d4tc03640a

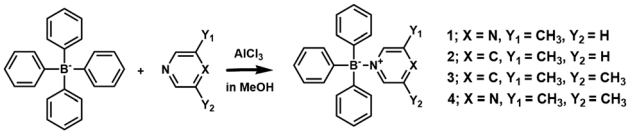

Fig. 1 Synthetic scheme of B ← N compounds and their chemical structures.

B ← N coordination compounds have attracted attention due to their easy synthesis, valid combination, and unique photophysical properties.[21] Among the boron compounds, BX_3 (X is F, Cl, or Br) and tris(pentafluorophenyl)borane (BCF) are commonly used. They act as strong Lewis acids, forming acid–base adducts by coordinating nitrogen-containing molecules to boron.[22] While extensive research has focused on optimizing the optical properties of B ← N compounds, no reported successes have demonstrated both photochromism and NIR photothermal conversion.

To achieve this goal, a series of simple B ← N compounds (Fig. 1) were prepared using tetraphenylborate and pyridine/pyrazine derivatives to effectively modulate the HOMO–LUMO band gap, enabling photochromation and application in photothermal conversion materials.

Results and discussion

Structural characterization

Compounds **1–4** were prepared by dissolving $NaBPh_4$, pyridine, or pyrazine derivatives in methanol. Then $AlCl_3$ was added, and the mixture was left for one day to give crystals. A single crystal X-ray structure analysis of **1** revealed the formation of B ← N bonds. Compound **1** crystallized in the $P2_1/c$ space group, and no solvent molecules were present in the crystal lattice (Fig. 2a and Fig. S1 and S2, ESI†). In the Lewis acid–base adducts (**1** and **4**) of pyrazine and BPh_3, the N(2) atom is not coordinated to boron due to steric hindrances caused by one or two methyl groups substituted for pyrazine. The N(2) of **1** interacts with the *para* hydrogen of the phenyl groups in two adjacent molecules (Fig. S1, ESI†). Compound **2** (Fig. 2b and Fig. S3, ESI†) was crystallized in the $P2_1/n$ space group with no significant interaction with neighboring molecules, and **3** (Fig. 2c and Fig. S4, ESI†) in the $P2_1/c$ space group, the latter being assembled in one-dimension (1D) with CH$\cdots\pi$ interactions along the *b* axis (Fig. S4 and S5, ESI†). Compound **4** (Fig. 2d), which has no solvent molecule, was crystallized in the $P2_1/c$ space group with $Z = 4$ and is assembled with C–H–π interactions along the *b*-axis (Fig. S6 and S7, ESI†). The bond lengths (d_{B-N}) of B–N in pyrazine adducts **1** and **4** (1.673(3) and 1.674(3) Å), and pyridine adducts **2** and **3** (1.666(4) and 1.662(3) Å) are very similar. Powder X-ray diffraction (PXRD) measurements agree well with the simulated pattern of a single crystal (Fig. S8, ESI†).

Photochromism

Compounds **2** and **3** did not change color when exposed to UV light (365 nm, 20 mW cm^{-2}), while **1** gradually changed from white to brown and **4** to dark brown (Fig. 3). Even when UV irradiation stops, compounds **1** and **4** do not return to their original colors for two weeks, indicating a high stability of photochromism (Fig. S9, ESI†). Upon UV irradiation, they exhibit a blue–green luminescence peak at 465 nm (λ_{ex} = 350 nm), gradually decreasing intensity with time (Fig. 3 and Fig. S10, ESI†). Compounds **2** and **3** show a luminescent maximum at 445 nm and 435 nm (λ_{ex} = 350 nm), respectively, and their spectra remained unchanged with time (Fig. S11, ESI†). The PXRD and IR measurements show that the compound's post-irradiation profile closely

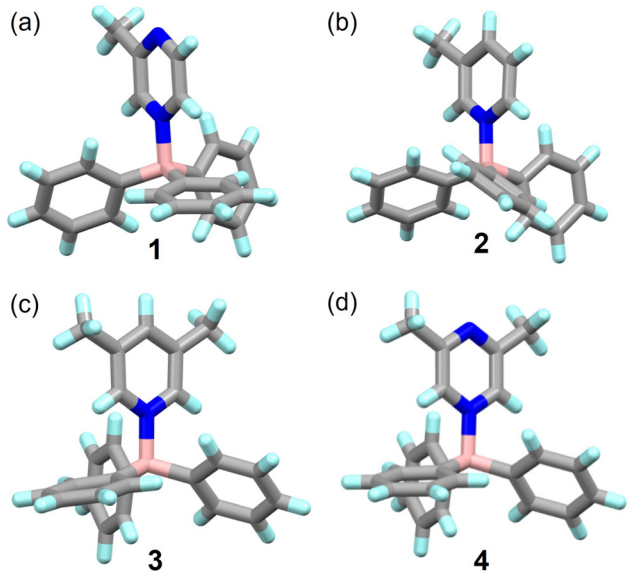

Fig. 2 Crystal structures of **1** (a), **2** (b), **3** (c) and **4** (d). Color codes: B, pale pink; C, grey; N, blue; C, gray; H, light blue.

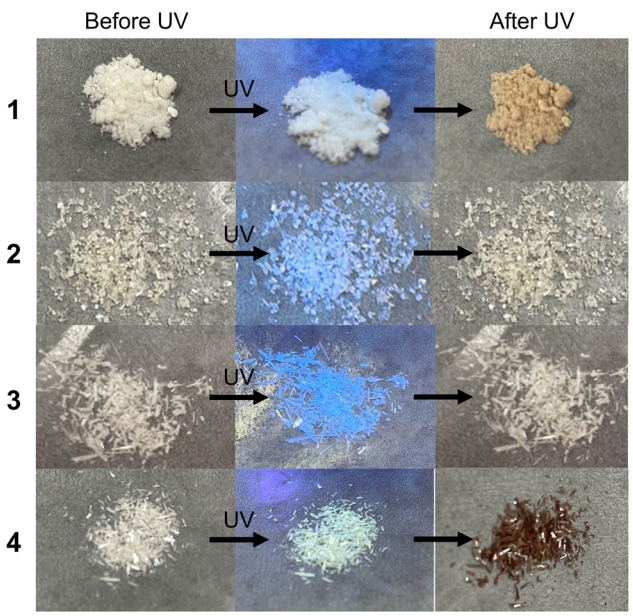

Fig. 3 Photographs of **1** (a), **2** (b), **3** (c), and **4** (d) before and after UV irradiation (365 nm).

resembles the pre-irradiation profile, indicating that no structural changes occur during the photochromic process (Fig. S12 and S13, ESI†).

The diffuse reflectance spectra of crystalline solid samples **1** and **4** were measured before and after UV irradiation and showed absorption bands at <400 nm for the former (Fig. 4a and b). The diffuse reflectance spectrum, measured upon UV irradiation (20 mW cm^{-2}), suggests that changes saturate in approximately one minute (Fig. S10, ESI†). After 10 minutes, they exhibited new broad absorption bands in the 400–1000 nm, suggesting the formation of pyrazine radicals, as indicated in previous literature.[23] As these results are often due to radical generation by electron transfer between donors and receptors, electron spin resonance (ESR) measurements were performed (Fig. 4c and d). A characteristic signal of organic radicals was observed in **1** and **4** before UV irradiation, suggesting the possibility of radical formation under ambient light. The strong ESR signals of **1**_UV and **4**_UV obtained after UV irradiation indicate increased organic radicals. The *g*-factors are 2.0002 for **1**_UV and 2.0014 for **4**_UV, respectively. Density functional theory (DFT) calculations were performed to gain insight into the photochromism of all compounds (Fig. 4e and f). The lowest unoccupied molecular orbital (LUMO) is found entirely on the pyridine or pyrazine group, while the electron distribution of the highest occupied molecular orbital (HOMO) is centered on the phenyl groups of triphenylborane. The electron-rich triphenylborane moiety and the electron-deficient pyridinium cation can be electron donors and acceptors, respectively. This chromic process is attributed to electron transfer (ET) from the phenyl group of triphenylborane to the pyrazine moiety, forming a pyrazine radical ($prz^{\bullet}$). According to the calculated orbital energy diagram, compounds **1** and **4** exhibit narrow energy gaps due to the reduced energy of the LUMO (Fig. 4e and Fig. S14, ESI†). This small energy gap decreases the enthalpy of the reaction, facilitating the excitation of electrons in the ground state when exposed to UV irradiation (365 nm).

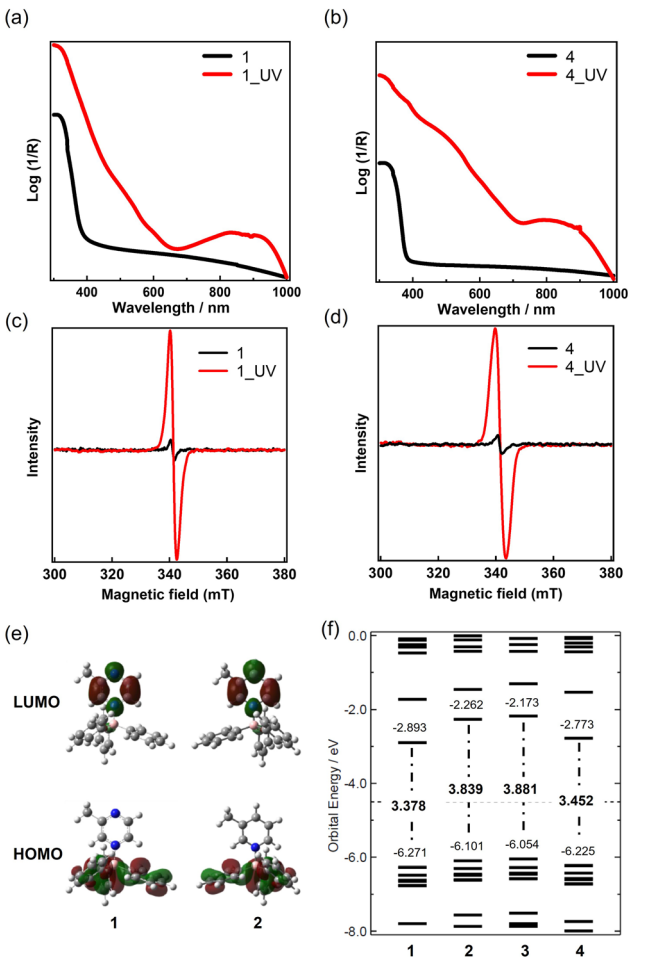

Fig. 4 Diffuse reflectance spectra of **1** (a) and **4** (b) before and after UV irradiation for 10 minutes. ESR spectra of **1** (c) and **4** (d) before and after UV irradiation for 10 minutes. HOMO/LUMO plots (e) and calculated orbital energy levels (f) of **1** and **2**.

To further confirm the presence of the pyrazine radical, we conducted X-ray photoelectron spectroscopy (XPS) measurements, focusing on compound **4** due to its high radical stability and structural similarity to compound **1**. The N 1s core-level spectrum of compound **4** showed a peak centered around a binding energy of 401.2 eV, indicating the presence of two components attributed to pyridine nitrogen atoms and positively charged nitrogen atoms (Fig. S15, ESI†). After light irradiation, a new, weak peak appeared at a lower binding energy of approximately 398.5 eV, previously assigned to the pyrazine radical,[14c,23a] indicating electron uptake by the pyrazine site. These findings support the presence of pyrazine radicals, as ESR studies and theoretical calculations suggested. IR and PXRD measurements indicated the absence of isomerization (Fig. S12 and S13, ESI†). Therefore, it is reasonable to conclude that the photochromism observed in compounds **1** and **4** is based on an electron transfer mechanism.

Radical stability in compounds **1** and **4** is thought to be achieved by inhibiting the reaction with atmospheric oxygen through the shielding effect[20d] in the crystalline state and the protective effect[24] of one or two methyl groups. The reason photochromism is observed in compounds **1** and **4**, but not in compounds **2** and **3**, is that pyrazine possesses a lower π–π* transition energy relative to pyridine (as confirmed by the calculated orbital energy diagram in Fig. 4f),[23b] a superior electron-accepting ability, and facilitates easier electron transfer. This characteristic has also been reported to lead to the formation of pyrazine radicals, which induce photochromism in pyrazine-based coordination compounds[23a] and organic–inorganic hybrid metal halides containing monoprotonated pyrazinium.[23b,23d]

Photothermal conversion

The IR camera recorded the photothermal conversion properties of all four compounds (Fig. 5a and b). When irradiated to a NIR laser (850 nm, 0.3 W cm^{-2}) for 5 minutes, these compounds exhibited weak photothermal conversion properties, with surface temperatures reaching up to 40 °C. In contrast, compounds **1**_UV and **4**_UV showed a rapid increase in surface temperature when irradiated with the same NIR laser. Specifically, the temperature for **1**_UV increased to 84 °C, while **4**_UV

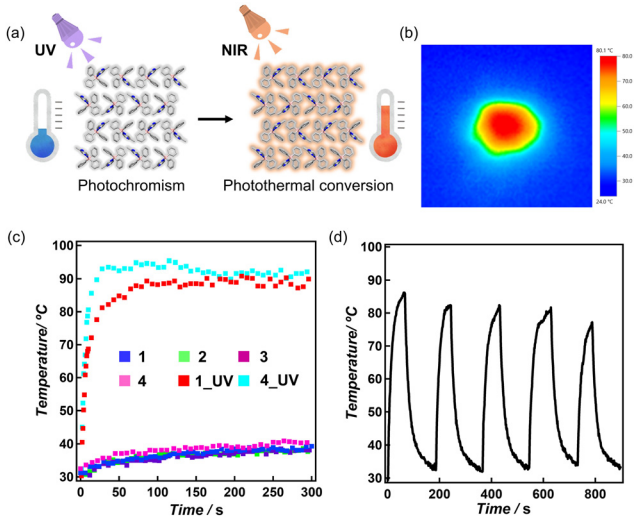

Fig. 5 (a) Schematic illustration of photothermal conversion enhanced by photochromism. (b) IR camera images of **4**_UV during NIR laser irradiation (850 nm, 0.3 W cm^{-2}). (c) Photothermal conversion curves upon UV light exposure (365 nm, 20 mW cm^{-2}) for 5 min. (d) Cyclic photothermal curve for **1**_UV upon NIR laser irradiation.

reached 93 °C within just one minute. This indicates that photochromism significantly enhances the photothermal conversion capabilities of these compounds. After continued exposure to the NIR light, the surface temperature remained nearly constant for approximately 4 minutes (Fig. 5c).

Although cyclic NIR photothermal conversion experiments of **1**_UV and **4**_UV do not show significant changes in the peak temperature, they gradually decrease with repeated experiments (Fig. 5d and Fig. S16, ESI†). This decrease appears to be due to the increase in the temperature of the compound, which causes quenching of the organic radicals generated. Additionally, PXRD analysis conducted before and after NIR irradiation at 0.3 W cm^{-2} for 10 minutes revealed that the crystallinity of the compound remained unchanged, indicating no structural decomposition resulting from NIR exposure (Fig. S8, ESI†). This suggests that the photothermal conversion properties can be fully restored through re-irradiation with UV light, even with repeated or prolonged use, which could lead to radical depletion. The photothermal conversion efficiency (η) during the initial NIR irradiation for **1**_UV and **4**_UV was calculated to be 66% and 82%, respectively, based on a time-$\ln(\theta)$ linear cooling curve (Fig. S17 and S18, ESI†). **4**_UV exhibited higher efficiency due to the more pronounced effect of electron donation from pyrazine, which has two methyl substituents. These efficiencies are remarkably high, surpassing many reported compounds such as Ag_2S (9.5%),[25] $Cu_{2-x}Se$ nanocrystals (22%),[26] Au nanorods (21%),[26] organic cocrystals (15.0%),[20b] perylenediimide-based supramolecular assemblies (31.6%)[13a] and MOFs (52.3%),[20d] Ag-CP (22.1%),[25] and viologen-based MOFs (77%).[20a]

Conclusions

Four Lewis adducts were prepared by combining pyridine/pyrazine derivatives with triphenylborane. Upon exposure to UV light, compounds **1** and **4**, which contain pyrazine derivatives, exhibited photochromism by luminescence quenching. Theoretical calculations showed that the low LUMO energy facilitates intramolecular electron transfer, leading to photochromism. Compounds **1**_UV and **4**_UV displayed highly efficient NIR photothermal conversion properties, outperforming previously reported inorganic compounds, organic covalent crystals, and MOF materials. These findings indicate that B ← N adducts not only allow for the creation of easily prepared new molecules but also suggest their potential use as optically functional materials through electron transfer.

Experimental

Materials and instruments

All chemicals and solvents used in the preparation were purchased from Tokyo Kasei Co and Wako Pure Chemical Industries, Ltd. and used without further purification. Compounds **1–4** were prepared according to the reported method with minor modifications.[27]

Syntheses of 1–4

Compound 1. 2-Methylpyrazine (0.019 g, 0.2 mmol), $NaBPh_4$ (0.068 g, 0.2 mmol), and $AlCl_3$ (0.027 g, 0.2 mmol) were mixed in methanol (50 mL) and allowed to stand for 1 day. This resulted in the formation of colorless plate-like crystals of **1** (Yield; 0.038 g, 57%). Anal. calcd for $C_{23}H_{21}BN_2{\cdot}0.5MeOH$: C, 80.13; H, 6.58; N, 7.95. Found: C, 80.05; H, 6.70; N, 7.93%.

Compound 2. Compound **2** was prepared using the same method as preparing **1**, except that 3-methylpyridine (0.018 g, 0.2 mmol) was used instead of 2-methylpyrazine. Colorless plate-like crystals of **2** (yield; 0.033 g, 49%). Anal. calcd for $C_{24}H_{22}BN{\cdot}0.5MeOH$: C, 83.77; H, 6.89; N, 3.99. Found: C, 83.60; H, 6.45; N, 4.03%.

Compound 3. Compound **3** was prepared using the same method as preparing **1**, except that 3,5-lutidine (0.021 g, 0.2 mmol) was used instead of 2-methylpyrazine. Colorless plate-like crystals of **3** (Yield; 0.036 g, 52%). Anal. calcd for $C_{25}H_{24}BN$: C, 85.97; H, 6.93; N, 4.01. Found: C, 85.62; H, 6.46; N, 3.18%.

Compound 4. Compound **4** was prepared using the same method as preparing **1**, except that 2,6-dimethylprazine (0.022 g, 0.2 mmol) was used instead of 2-methylpyrazine. Colorless plate-like crystals of **4** (yield; 0.032 g, 45%). Anal. calcd for $C_{24}H_{23}BN_2{\cdot}0.3MeOH$: C, 81.30; H, 6.78; N, 7.78. Found: C, 81.11; H, 6.18; N, 7.99%.

Physical measurements

X-ray diffraction data of single-crystals **1–4** were collected using a Rigaku Saturn 70. The structures were determined by direct methods (SHELXT[28]) and refined with the SHELXL program using full-matrix least-squares refinement.[29] Hydrogen atoms were refined geometrically using a riding model. Detailed crystallographic data are summarized in Table S1 (ESI†). ESR spectra were recorded using a JEOL JES-RE3X electron spin

resonance paramagnetic spectrometer. Photothermal conversion data were recorded using a Testo-871. Diffuse reflectance spectra were measured on a JASCO model V-670 UV/Vis spectrophotometer equipped with an integrating-sphere unit ISN-723.

Computational methods

DFT calculations were performed using the B3LYP functional and the 6-31G(d) basis set. All calculations were conducted with the Gaussian16 program,[30] and the results were visualized using GaussView software.[31]

Data availability

All relevant data have been included in the paper and ESI.†

Author contributions

S. K. and Y. K. supervised this study. T. M. carried out the experimental work and analyzed the data. K. R. provided advice on the synthesis method of the compounds. M. S. and M. K. conducted the measurement of photothermal conversion. T. F. collected the Diffuse reflectance spectroscopic data. N. H. performed the theoretical calculations. T. I. collected the ESR data. Y. K. assisted in scientific discussions. All the authors contributed to the writing of the manuscript.

Conflicts of interest

There are no conflicts to declare.

Acknowledgements

This work was supported by KAKENHI Grant Number JP22K14698. This work was also supported by the Grant-in-Aid for Transformative Research Areas (A) ''Supra-ceramics'' (JSPS KAKENHI Grant Number JP23H04636, JP23H04614 and JP 23H04617).

References

1 (*a*) X. Huang, I. H. El-Sayed, W. Qian and M. A. El-Sayed, *J. Am. Chem. Soc.*, 2006, **128**, 2115–2120; (*b*) L. Cheng, C. Wang, L. Feng, K. Yang and Z. Liu, *Chem. Rev.*, 2014, **114**, 10869–10939.

2 (*a*) L. Dykman and N. Khlebtsov, *Chem. Soc. Rev.*, 2012, **41**, 2256–2282; (*b*) S. S. Kelkar and T. M. Reineke, *Bioconjugate Chem.*, 2011, **22**, 1879–1903.

3 (*a*) P. K. Jain, X. Huang, I. H. El-Sayed and M. A. El-Sayed, *Acc. Chem. Res.*, 2008, **41**, 1578–1586; (*b*) N. Rohaizad, C. C. Mayorga-Martinez, M. Fojtu, N. M. Latiff and M. Pumera, *Chem. Soc. Rev.*, 2021, **50**, 619.

4 H. S. Jung, P. Verwilst, A. Sharma, J. Shin, J. L. Sessler and J. S. Kim, *Chem. Soc. Rev.*, 2018, **47**, 2280–2297.

5 (*a*) H.-J. Yoon, H.-S. Lee, J.-Y. Lim and J.-H. Park, *ACS Appl. Mater. Interfaces*, 2017, **9**, 5683–5691; (*b*) Z. Chen, P. Zhao, Z. Luo, M. Zheng, H. Tian, P. Gong, G. Gao, H. Pan, L. Liu, A. Ma, H. Cui, Y. Ma and L. Cai, *ACS Nano*, 2016, **10**, 10049.

6 (*a*) L. Cheng, W. He, H. Gong, C. Wang, Q. Chen, Z. Cheng and Z. Liu, *Adv. Funct. Mater.*, 2013, **23**, 5893; (*b*) S. Luo, X. Tan, S. Fang, Y. Wang, T. Liu, X. Wang, Y. Yuan, H. Sun, Q. Qi and C. Shi, *Adv. Funct. Mater.*, 2016, **26**, 2826.

7 (*a*) B. Zhou, Y. Li, G. Niu, M. Lan, Q. Jia and Q. Liang, *ACS Appl. Mater. Interfaces*, 2016, **8**, 29899; (*b*) H. S. Jung, J.-H. Lee, K. Kim, S. Koo, P. Verwilst, J. L. Sessler, C. Kang and J. S. Kim, *J. Am. Chem. Soc.*, 2017, **139**, 9972.

8 (*a*) C. S. Jin, J. F. Lovell, J. Chen and G. Zheng, *ACS Nano*, 2013, **7**, 2541–2550; (*b*) O. Taratula, C. Schumann, T. Duong, K. L. Taylor and O. Taratula, *Nanoscale*, 2015, **7**, 3888–3902.

9 (*a*) C. S. Jin, J. F. Lovell, J. Chen and G. Zheng, *ACS Nano*, 2013, **7**, 2541–2550; (*b*) Q. Zou, M. Abbas, L. Zhao, S. Li, G. Shen and X. Yan, *J. Am. Chem. Soc.*, 2017, **139**, 1921–1927.

10 (*a*) Y. Cai, P. Liang, Q. Tang, X. Yang, W. Si, W. Huang, Q. Zhang and X. Dong, *ACS Nano*, 2017, **11**, 1054–1063; (*b*) K. Pu, J. Mei, J. V. Jokerst, G. Hong, A. L. Antaris, N. Chattopadhyay, A. J. Shuhendler, T. Kurosawa, Y. Zhou, S. S. Gambhir, Z. Bao and J. Rao, *Adv. Mater.*, 2015, **27**, 5184–5190.

11 (*a*) G. T. Spence, G. V. Hartlanda and B. D. Smith, *Chem. Sci.*, 2013, **4**, 4240–4244; (*b*) G. T. Spence, S. S. Lo, C. Ke, H. Destecroix, A. P. Davis, G. V. Hartland and B. D. Smith, *Chem. – Eur. J.*, 2014, **20**, 12628–12635.

12 G. Chen, J. Sun, Q. Peng, Q. Sun, G. Wang, Y. Cai, X. Gu, Z. Shuai and B. Z. Tang, *Adv. Mater.*, 2020, **32**, 1908537.

13 (*a*) C. M. Zhang, M. N. A. S. Ivan, Y. Sun, Z. Li, S. Saha, S. Ahmed, H. Liu, Y. Wang, Y. H. Tsang and W. Y. Wong, *J. Mater. Chem. A*, 2024, **12**, 9055–9065; (*b*) Y. Cao, J.-H. Dou, N.-J. Zhao, S. Zhang, Y.-Q. Zheng, J.-P. Zhang, J.-Y. Wang, J. Pei and Y. Wang, *Chem. Mater.*, 2017, **29**, 718–725; (*c*) T. Yang, L. Liu, Y. Deng, Z. Guo, G. Zhang, Z. Ge, H. Ke and H. Chen, *Adv. Mater.*, 2017, **29**, 1700487.

14 (*a*) H.-Y. Li, Y.-L. wie, X.-Y. Dong, S.-Q. Zang and T. C. W. Mak, *Chem. Mater.*, 2015, **27**, 1327–1331; (*b*) G. Xu, G.-C. Guo, M.-S. Wang, Z.-J. Zhang, W.-T. Chen and J.-S. Huang, *Angew. Chem., Int. Ed.*, 2007, **46**, 3249–3251; (*c*) X.-Y. Lv, M.-S. Wang, C. Yang, G.-E. Wang, S.-H. Wang, R.-G. Lin and G.-C. Guo, *Inorg. Chem.*, 2012, **51**, 4015–4019.

15 (*a*) C. Zhang, L. Sun, Y. Yan, Y. Liu, Z. Liang, Y. Liu and J. Li, *J. Mater. Chem. C*, 2017, **5**, 2084–2089; (*b*) W. An, D. Aulakh, X. Zhang, W. Verdegaal, K. R. Dunbar and M. Wriedt, *Chem. Mater.*, 2016, **28**, 7825–7832; (*c*) W.-Q. Kan, S.-Z. Wen, Y.-C. He and C.-Y. Xu, *Inorg. Chem.*, 2017, **56**, 14926–14935.

16 (*a*) P. Ma, F. Hu, J. Wang and J. Niu, *Coord. Chem. Rev.*, 2019, **378**, 281–309; (*b*) K. Hakouk, O. Oms, A. Dolbecq, H. E. Moll, J. Marrot, M. Evain, F. Molton, C. Duboc, P. Deniard, S. Jobic, P. Mialane and R. Dessapt, *Inorg. Chem.*, 2013, **52**, 555–557.

17 (*a*) A. R. Y. Almuhana, G. R. F. Orton, C. Rosenberg and N. R. Champness, *Chem. Commun.*, 2024, **60**, 452–455; (*b*) S. Masuda, S. Kusumoto, M. Okamura, S. Hikichi, R. Tokunaga, S. Hayami, Y. Kim and Y. Koide, *Dalton Trans.*, 2023, **52**, 10531–10536.

18 (*a*) D. Schmidt, D. Bialas and F. Wűrthner, *Angew. Chem., Int. Ed.*, 2015, **54**, 3611–3614; (*b*) R. O. Marcon and S. Brochsztain, *Langmuir*, 2007, **23**, 11972–11976; (*c*) Y. Jiao, K. Liu, G. Wang, Y. Wang and X. Zhang, *Chem. Sci.*, 2015, **6**, 3975–3980.

19 (*a*) J. Zhang, Q. Zou and H. Tian, *Adv. Mater.*, 2013, **25**, 378–399; (*b*) M. Irie, *Chem. Rev.*, 2000, **100**, 1685–1716; (*c*) J. A. Delaire and K. Nakatani, *Chem. Rev.*, 2000, **100**, 1817–1845; (*d*) N. Tamai and H. Miyasaka, *Chem. Rev.*, 2000, **100**, 1875–1890.

20 (*a*) S. Wang, S. Li, J. Xiong, Z. Lin, W. Wei and Y. Xu, *Chem. Commun.*, 2020, **56**, 7399–7402; (*b*) D. Wang, X. Kan, C. Wu, Y. Gong, G. Guo, T. Liang, L. Wang, Z. Li and Y. Zhao, *Chem. Commun.*, 2020, **56**, 5223–5226; (*c*) B. Tang, W.-L. Li, Y. Chang, B. Yuan, Y. Wu, M.-T. Zhang, J.-F. Xu, J. Li and X. Zhang, *Angew. Chem.*, 2019, **131**, 15672–15677; (*d*) B. Lü, Y. Chen, P. Li, B. Wang, K. Müllen and M. Yin, *Nat. Commun.*, 2019, **10**, 767; (*e*) S. Park, J. Lee, H. Jeong, S. Bae, J. Kang, D. Moon and J. Park, *Chemistry*, 2022, **8**, 1993–2010.

21 (*a*) G. Campillo-Alvarado, K. P. D'mello, D. C. Swenson, S. V. Santhana Mariappan, H. Hçpfl, H. Morales-Rojas and L. R. MacGillivray, *Angew. Chem., Int. Ed.*, 2019, **58**, 5413–5416; (*b*) W. Wang, L. Wang, F. Du, G.-D. Wang, L. Hou, Z. Zhu, B. Liu and Y.-Y. Wang, *Chem. Sci.*, 2023, **14**, 533–539; (*c*) T. Ono, Y. Tsukiyama, S. Hatanaka, Y. Sakatsume, T. Ogoshi and Y. Hisaeda, *J. Mater. Chem. C*, 2019, **7**, 9726–9734; (*d*) G. Campillo-Alvarado, R. J. Liu, D. W. Davies and Y. Diao, *Cryst. Growth Des.*, 2021, **21**, 3143–3147.

22 (*a*) J. Huang, X. Wang, Y. Xiang, L. Guo and G. Chen, *Adv. Energy Sustainability Res.*, 2021, **2**, 2100016; (*b*) L. Guo, K. Liu, X. Tan, X. Wang, J. Huang, Z. Wei and G. Chen, *Macromolecules*, 2021, **54**, 10758–10766; (*c*) S. Hatanaka, T. Ono, Y. Yano, D. T. Gryko and Y. Hisaeda, *ChemPhotoChem*, 2020, **4**, 138–143.

23 (*a*) X. Zhang, M.-S. Wang, C. Sun, C. Yang, P.-X. Li and G.-C. Guo, *Chem. Commun.*, 2016, **52**, 7947–7949; (*b*) P. Hao, H. Li, T. Yu and Y. Fu, *Dyes Pigm.*, 2017, **136**, 825–829; (*c*) A. N. Singh, P. N. Balasubramanian and E. S. Gould, *Inorg. Chem.*, 1983, **22**, 655–661; (*d*) T.-L. Yua, Y.-M. Guo, G.-X. Wu, X.-F. Yang, M. Xue, Y.-L. Fu and M.-S. Wang, *Coord. Chem. Rev.*, 2019, **397**, 91–111.

24 I. Ratera and J. Veciana, *Chem. Soc. Rev.*, 2012, **41**, 303–349.

25 M.-Q. Li, M. Zhao, L.-Y. Bi, Y.-Q. Hu, G. Gou, J. Li and Y.-Z. Zheng, *Inorg. Chem.*, 2019, **58**, 6601–6608.

26 C. M. Hessel, V. P. Pattani, M. Rasch, M. G. Panthani, B. Koo, J. W. Tunnell and B. A. Korgel, *Nano Lett.*, 2011, **11**, 2560–2566.

27 Y. Hashimoto, A. Nagai, T. Banno and M. Umeno, *JP. Pat.*, JP2003238572, 2003.

28 G. M. Sheldrick, *Acta Crystallogr., Sect. A: Found. Adv.*, 2015, **71**, 3–8.

29 G. M. Sheldrick, *Acta Crystallogr., Sect. C: Struct. Chem.*, 2015, **71**, 3–8.

30 M. J. Frisch, G. W. Trucks, H. B. Schlegel, G. E. Scuseria, M. A. Robb, J. R. Cheeseman, G. Scalmani, V. Barone, G. A. Petersson, H. Nakatsuji, X. Li, M. Caricato, A. V. Marenich, J. Bloino, B. G. Janesko, R. Gomperts, B. Mennucci, H. P. Hratchian, J. V. Ortiz, A. F. Izmaylov, J. L. Sonnenberg, D. Williams-Young, F. Ding, F. Lipparini, F. Egidi, J. Goings, B. Peng, A. Petrone, T. Henderson, D. Ranasinghe, V. G. Zakrzewski, J. Gao, N. Rega, G. Zheng, W. Liang, M. Hada, M. Ehara, K. Toyota, R. Fukuda, J. Hasegawa, M. Ishida, T. Nakajima, Y. Honda, O. Kitao, H. Nakai, T. Vreven, K. Throssell, J. A. Montgomery, Jr., J. E. Peralta, F. Ogliaro, M. J. Bearpark, J. J. Heyd, E. N. Brothers, K. N. Kudin, V. N. Staroverov, T. A. Keith, R. Kobayashi, J. Normand, K. Raghavachari, A. P. Rendell, J. C. Burant, S. S. Iyengar, J. Tomasi, M. Cossi, J. M. Millam, M. Klene, C. Adamo, R. Cammi, J. W. Ochterski, R. L. Martin, K. Morokuma, O. Farkas, J. B. Foresman and D. J. Fox, *Gaussian 16, Revision A.03*, Gaussian, Inc., Wallingford CT, 2016.

31 R. Dennington, T. A. Keith and J. M. Millam, *Gauss View, Version 6*, Semichem Inc., Shawnee Mission, KS, 2016.